Romanian Reports in Physics, Vol. 59, No. 2, P. 387–396, 2007

Dedicated to Prof. Dorin N. Poenaru's 70th Anniversary

MACROSCOPIC POTENTIAL ENERGY SURFACES OF HEAVY AND SUPERHEAVY NUCLEI

CRISTINA CÎRTOAJE[1], ILEANA-HANIA PLONSKI[2]

[1] *"Politehnica" University, Bucharest, Romania*
E-mail: cristina_cirtoaje@physics.pub.ro
[2] *"Horia Hulubei" National Institute for Nuclear Physics and Engineering*
P.O. Box MG-6, RO-077125 Bucharest-Magurele, Romania
E-mail: plonski@ifin.nipne.ro

(Received February 17, 2007)

Abstract. Potential energy surfaces of heavy and superheavy nuclei function of the separation distance of the fragments and the mass-asymmetry are calculated within the Yukawa-plus-exponential phenomenological model, by using the nuclear surface parametrization of two intersected spheres. The fusion barrier height and the saddle-point position are studied for 200 even-even compound nuclei with atomic numbers $Z = 90 - 104$ and neutron numbers $N = 128 - 176$. When the mass number increases along the line of beta-stability, the barrier height decreases from 23.89 MeV to 10.34 MeV. The saddle-point position of the majority of nuclides lies outside the touching-point configuration (separated fragments); it moves inside (overlapping participants) for heavier nuclei.

Key words: heavy nuclei, macroscopic energy, potential energy surfaces, fusion barriers.

1. INTRODUCTION

From 1939 to 1967 the phenomenological liquid drop model (LDM) was used to explain nuclear fission and fusion phenomena. The analogy between nuclear matter and a uniformly charged liquid drop is suggested by the saturation properties: both nuclear density and average binding energy per particle are approximately the same for all nuclei, except the lightest ones. The nuclear matter has a low compressibility and the nucleus posses a well-defined surface.

Already in 1933, Wolfgang Pauli addressed to Werner Heisenberg the question "Why the nucleus should be built in analogy to the liquid drop,

and not to the crystalline state?" His answer was [1] "From the empirical energy differences in nuclear spectra one may deduce the order of magnitude of the momenta with which neutrons and protons move in the nucleus ($p^2/2M \sim \Delta E$). If one calculates from them the dimensions of the orbits according to $\Delta q \sim \hbar/p$, then Δq empirically becomes of the order of the nuclear dimension, i.e. the individual particles circulate in the whole nucleus and do not just oscillate around an equilibrium position. The deeper reason must lie in the neutron-proton force law". Since the binding energy of the deuteron was approximately known ($\Delta E = 2.23$ MeV), it was possible to estimate Δq, i.e. the size of the deuteron, from which the range of the nuclear forces follows approximately as $r_0 \sim \Delta q/2 \sim 1.5 \times 10^{-13}$ cm.

Fission of highly excited nuclei in the intermediate mass region is dominated by the liquid drop properties of nuclear matter. A unified approach of light particle evaporation and fission decay modes of highly excited compound nuclei well above the barrier height, was developed by Moretto [2] who applied the transition state formalism used in fission to the light particle evaporation.

Particularly successful variant of the LDM was introduced by Myers and Swiatecki [3]. Nevertheless, the leptodermous expansion assumed in the LDM is only valid if all dimensions of the drop are large compared to the surface thickness, condition not satisfied for strongly necked-in configurations. Other deficiencies of the LDM surface energy are: the absence of attraction between separated nuclei at a small distance within the range of nuclear forces and the neglect of the surface diffusivity. To overcome these difficulties, the surface energy has been replaced by a folded Yukawa-plus-exponential potential (Y+EM) [4, 5]. The model was generalized for different charge densities of the fragments [6, 7, 8].

At low excitation energies one should also take into account a microscopic shell and pairing correction [9, 8], as it was recently done to calculate potential energy surfaces (PES) for cluster emitters [10] and for light and superheavy alpha emitters [11], by using the most advanced asymmetric two center shell model [12, 13, 14].

Based on the LDM, in 1939 Lise Meitner understood that very heavy nuclei (with atomic number over about 100) would never exist because there would be no potential barrier against spontaneous decay. The LDM fission barrier height of the very heavy nuclides is very small: $B_f < 0.4$ MeV for $Z \geq 110$, $B_f < 0.05$ MeV for $Z \geq 114$, and $B_f = 0$ for $Z \geq 122$. This fission property has been taken to be a good explanation why superheavy elements could not be found in nature, until the macroscopic-microscopic method was developed [9].

The purpose of the present work is to study how the Y+EM fusion barrier height and position is changed when the mass number of the parent nucleus is increased.

2. THE MODEL

The simplest parametrization of the nuclear surface for a binary fusing system of nuclei

$$ {}^{A_1}Z_1 + {}^{A_2}Z_2 \rightarrow {}^{A}Z, \quad A_1 + A_2 = A, \quad Z_1 + Z_2 = Z \tag{1} $$

is that of two intersected spheres, with radii $R_i = r_0 A_i^{1/3}$ fm, where the nuclear radius constant is $r_0 = 1.16$ fm. For a binary fission process one may keep constant one of the radius (e.g. R_2) and take as a deformation coordinate the separation distance between the two spheres, R, whose initial value is $R_i = R_0 - R_2$ and at the touching point (two tangent spheres) it is $R_t = R_1 + R_2$. Two convenient parameters of deformation could be the dimensionless separation distance, ξ, and the mass asymmetry η defined by

$$ \xi = \frac{R - R_i}{R_t - R_i}, \quad \eta = \frac{A_1 - A_2}{A_1 + A_2}. \tag{2} $$

For a given mass asymmetry, η, at every separation distance, R, the unknown radius, R_1 is found from the volume conservation condition ($V_1 + V_2 = 4\pi R_0^3/3$).

By requesting zero deformation energy for a spherical shape, the potential energy is defined as

$$ E_{Y+EM} = (E_Y - E_Y^0) + (E_c - E_c^0) = E_Y^0 [B_Y - 1 + 2X(B_c - 1)], \tag{3} $$

where $E_Y^0 = a_2 A^{2/3}\{1 - 3x^2 + (1 + 1/x)[2 + 3x(1 + x)]\exp(-2/x)\}$, $E_c^0 = a_c Z^2 A^{-1/3}$ are energies corresponding to spherical shape and $a_2 = a_s(1 - \kappa I^2)$, $I = (N - Z)/A$, $x = a/R_0$, $R_0 = r_0 A^{1/3}$. The parameters $a_s, \kappa, a_c = 3e^2/(5r_0)$, and r_0 are taken from Möller et al. [15].

The relative Yukawa and Coulomb energies $B_Y = E_Y/E_Y^0$, $B_c = E_c/E_c^0$ are functions of the nuclear shape. The dependence on the neutron and proton numbers is contained in E_Y^0, in the fissility parameter $X = E_c^0/(2E_Y^0)$ and B_Y. For a binary fragmentation with charge densities ρ_{1e} and ρ_{2e}, one has [7] a relative energy

$$ B_Y = \frac{E_Y}{E_Y^0} = \frac{a_{21}}{a_{20}} B_{Y1} + \frac{\sqrt{a_{21}a_{22}}}{a_{20}} B_{Y12} + \frac{a_{22}}{a_{20}} B_{Y2}, \tag{4} $$

with axially-symmetric shape-dependent terms expressed by triple integrals

$$B_{Y1} = b_Y \int_{-1}^{x_c} dx \int_{-1}^{x_c} dx' \int_0^1 dw F_1 F_2 Q_Y, \tag{5}$$

$$B_{Y12} = b_Y \int_{-1}^{x_c} dx \int_{x_c}^{1} dx' \int_0^1 dw F_1 F_2 Q_Y, \tag{6}$$

$$B_{Y2} = b_Y \int_{x_c}^{1} dx \int_{x_c}^{1} dx' \int_0^1 dw F_1 F_2 Q_Y, \tag{7}$$

in which $b_Y = -d^4(r_0/2a^2)a_2 R_0 A/E_Y^0$, $d = (z'' - z')/2R_0$ is the nuclear semilength in units of R_0 and

$$F_1 = y^2 + yy_1 \cos\varphi - \frac{x - x'}{2}\frac{dy^2}{dx}, \tag{8}$$

$$\begin{aligned} Q_Y = \; & \{[\sqrt{P}(\sqrt{P} + 2a/R_0 d) + 2a^2/(R_0 d)^2] \cdot \\ & \cdot \exp(-R_0\sqrt{P}d/a) - 2a^2/(R_0 d)^2\}/P^2. \end{aligned} \tag{9}$$

F_2 is obtained from F_1 by replacing dy^2/dx with dy_1^2/dx'. In the above equations $P = y^2 + y_1^2 - 2yy_1\cos\varphi + (x - x')^2$, $w = \varphi/2\pi$, and x_c is the position of separation plane between fragments with -1, $+1$ intercepts on the symmetry axis (surface equation $y = y(x)$ or $y_1 = y(x')$). The integrals are computed numerically by Gauss-Legendre quadratures.

In a similar way the Coulomb relative energy is given by

$$B_c = \frac{E_c}{E_c^0} = \left(\frac{\rho_{1e}}{\rho_{0e}}\right)^2 B_{c1} + \frac{\rho_{1e}\rho_{2e}}{\rho_{0e}^2} B_{c12} + \left(\frac{\rho_{2e}}{\rho_{0e}}\right)^2 B_{c2} \tag{10}$$

and for axially symmetric shapes

$$B_{c1} = b_c \int_{-1}^{x_c} dx \int_{-1}^{x_c} dx' F(x, x'), \tag{11}$$

$$B_{c12} = b_c \int_{-1}^{x_c} dx \int_{x_c}^{1} dx' F(x, x'), \tag{12}$$

$$B_{c2} = b_c \int_{x_c}^{1} dx \int_{x_c}^{1} dx' F(x, x'), \tag{13}$$

where $b_c = 5d^5/8\pi$. In the integrand

$$\begin{aligned} F(x, x') = & \left\{ yy_1[(K - 2D)/3]\left[2(y^2 + y_1^2) - (x - x')^2 + \frac{3}{2}(x - x')\left(\frac{dy_1^2}{dx'} - \frac{dy^2}{dx}\right)\right] + \right. \\ & \left. + K\left\{ y^2 y_1^2/3 + \left[y^2 - \frac{x - x'}{2}\frac{dy^2}{dx}\right]\left[y_1^2 - \frac{x - x'}{2}\frac{dy_1^2}{dx'}\right]\right\}\right\} a_\rho^{-1}. \end{aligned} \tag{14}$$

K and K' are the complete elliptic integrals of the first and second kind, respectively:

$$K(k) = \int_0^{\pi/2} (1 - k^2 \sin^2 t)^{-1/2} dt, \tag{15}$$

$$K'(k) = \int_0^{\pi/2} (1 - k^2 \sin^2 t)^{1/2} dt, \tag{16}$$

and $a_\rho^2 = (y + y_1)^2 + (x - x')^2$, $k^2 = 4yy_1/a_\rho^2$, $D = (K - K')/k^2$. The elliptic integrals may be calculated by using Chebyshev polynomial approximation. For $x = x'$ the function F is not determined. In this case, after removing the indetermination, we get $F(x, x') = 4y^3/3$.

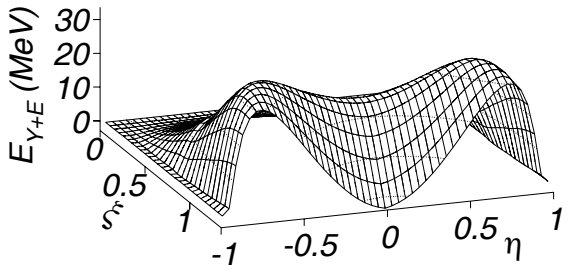

Fig. 1 – Y+EM potential energy surface *versus* $\xi = (R - R_i)/(R_t - R_i)$ and $\eta = (A_1 - A_2)/A$ for ^{230}Th nucleus.

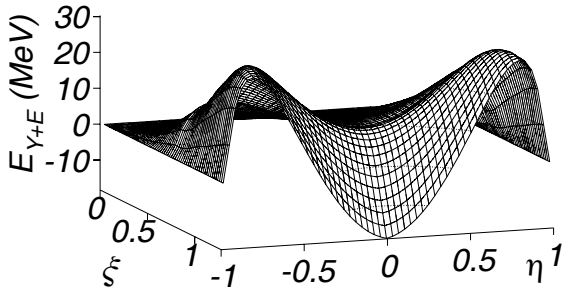

Fig. 2 – Y+EM potential energy surface *versus* $\xi = (R - R_i)/(R_t - R_i)$ and $\eta = (A_1 - A_2)/A$ for ^{262}Rf nucleus.

Starting from the touching point configuration, $R \geq R_t$, for spherical shapes of the fragments, one can use *analytical relationships.* The Coulomb interaction energy of a system of two spherical nuclei, separated by a distance R between centers, is $E_{c12} = e^2 Z_1 Z_2 / R$, where e is the electron charge.

Within a liquid drop model (LDM) there is no contribution of the surface energy to the interaction of the separated fragments; the barrier has a

maximum at the touching point configuration. The proximity forces acting at small separation distances (within the range of strong interactions) give rise in the Y+EM to an interaction term expressed as folllows

$$E_{Y12} = -4\left(\frac{a}{r_0}\right)^2 \sqrt{a_{21}a_{22}}\frac{\exp(-R/a)}{R/a}\left[g_1 g_2\left(4+\frac{R}{a}\right) - g_2 f_1 - g_1 f_2\right], \quad (17)$$

where

$$g_k = \frac{R_k}{a}\cosh\left(\frac{R_k}{a}\right) - \sinh\left(\frac{R_k}{a}\right), \quad (18)$$

$$f_k = \left(\frac{R_k}{a}\right)^2 \sinh\left(\frac{R_k}{a}\right). \quad (19)$$

In many cases the interaction energy is maximum at a certain distance $R_m > R_t = R_1 + R_2$, which can be found by solving numerically the following nonlinear equation

$$e^x + p_1 + x(p_1 + xp) = 0; \quad x = R/a \quad (20)$$

in which

$$p = -\frac{a^3}{r_0^2}\sqrt{a_{21}a_{22}}\frac{g_1 g_2}{e^2 Z_1 Z_2} \quad (21)$$

$$p_1 = p(4 - f_1/g_1 - f_2/g_2) \quad (22)$$

and the interval $x_t = R_t/a, x_t + 5$ may be given as input data of a program using Müller's iteration scheme of succesive bisections and inverse parabolic interpolation.

3. **RESULTS**

We performed calculations for 200 even-even nuclides with proton numbers $Z = 90-104$ and neutron numbers from $N = 128$ to $N = 176$. Two examples are given in Figs. 1 for ^{230}Th and 2 for ^{262}Rf parent (or compound) nuclei.

On both potential energy surfaces one can see a deep valley at symmetry ($\eta = 0$) and the Businaro-Gallone mountains at large deformations. The detailed shapes of the potential barrier along this valley are obtained as a cut of the PES at $\eta = 0$ and is represented in Fig. 3.

The position of the saddle-point (maximum value along these minima) lies at a dimensionless separation distance $\xi_{SP} = (R_{SP} - R_i)/(R_t - R_i)$ larger than unity for not very heavy nuclei (e.g. ^{230}Th) but starting from some large value of Z at smaller value of N, as shown in Fig. 4, $\xi_{SP} < 1$.

For a large number of heavy nuclei we have studied, the saddle point position remains almost constant around a value $\xi_{SP} \approx 1.06$. Then, for $Z = 100$ we found $\xi_{SP} < 1$ for nuclei with $N = 128 - 140$, for $Z = 102$

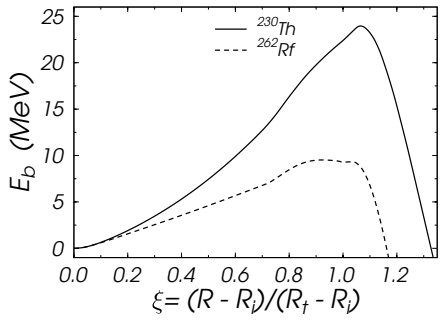

Fig. 3 – Y+EM potential barrier versus $\xi = (R - R_i)/(R_t - R_i)$ for symmetric binary fusion ($\eta = 0$) leading to ^{230}Th and ^{262}Rf compound nuclei.

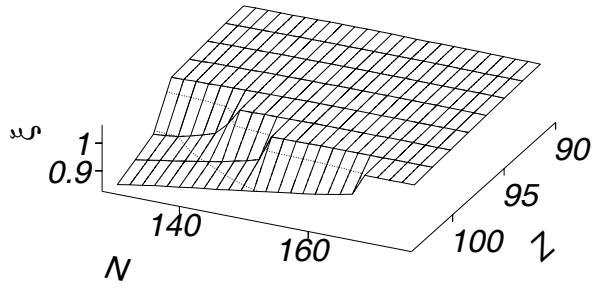

Fig. 4 – Surface plot of the saddle-point position $\xi_{SP} = (R_{SP} - R_i)/(R_t - R_i)$ versus the neutron and proton numbers of heavy nuclei.

the range is increased up to $N = 148$, and for $Z = 104$ the largest N with $\xi_{SP} < 1$ becomes $N = 166$.

For the nuclei under consideration, a maximum value of the fusion barrier height as large as $E_b = 24.97$ MeV is obtained for ^{244}Th, i.e. $Z = 90$, $N = 154$, as can be seen in Figs. 5 and 6. When the atomic number is increased up to 104 the barrier height decreases down to 3.45 MeV for ^{232}Rf ($Z = 104$, $N = 128$).

In order to see better the detailed variation with N and Z of the potential barrier height (Figs. 5 and 6) and the saddle-point position (Fig. 4) one may choose two different paths in the plane (N, Z): (1) variation with N along the Green approximation of the beta stability line

$$N - Z = 0.4A^2/(200 + A) \tag{23}$$

and (2) the variation with Z for the minimum value of N considered by us, which is $N_{min} = 128$. The results are plotted on the left-hand side of Fig. 7 for the former case and on the right-hand side for the latter.

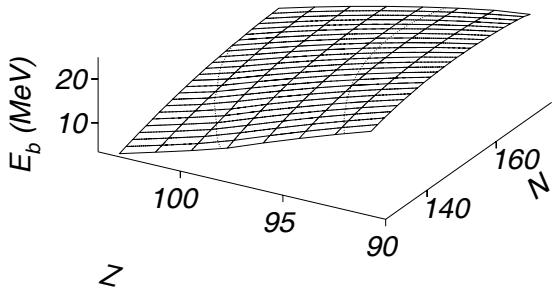

Fig. 5 – Surface plot of the barrier height versus the neutron and proton numbers of heavy nuclei.

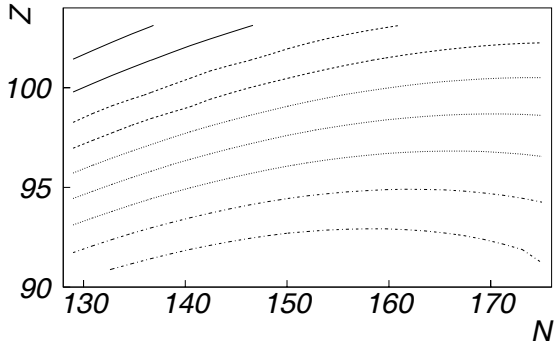

Fig. 6 – Contour plot of the barrier height versus the neutron and proton numbers of heavy nuclei.

When the neutron number along the line of beta stabilty is increased from 138 to 166 (from $Z = 90$ to $Z = 104$) the barrier height decreases almost linearly from 23.89 to 10.34 MeV. In the same time the position of the saddle-point decreases smoothly from 1.065 at $N = 138$ to 1.038 at $N = 162$ and suddenly decreases to 0.955 at $N = 164$.

On the right-hand side of Fig. 7 the lowest values of the barrier height at a given Z are obtained at $N = 128$. They are decreasing almost linearly from 21.97 MeV at $Z = 90$ to 3.45 MeV at $Z = 104$. The position of the saddle point decreases slowly from 1.063 at $Z = 90$ to 1.037 at $Z = 98$ and then there is a sudden jump to 0.891 at $Z = 100$ and finally less steeper to 0.833 at $Z = 104$.

In conclusion the macroscopic fusion barrier height decreases smoothly for heavier and heavier compund nuclei and the position of the saddle point remains in the region of separated fragments outside the touching point configuration ($\xi_{SP} > 1$) up to $Z = 98 - 104$ depending on the neutron number;

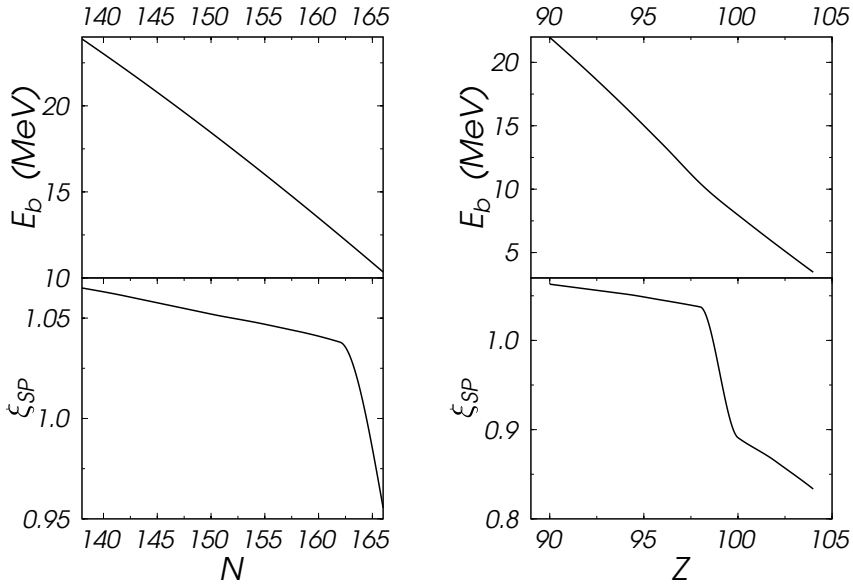

Fig. 7 – Barrier height (top-left) and position of the saddle-point (bottom-left) versus the neutron numbers of heavy nuclei along the beta stability line. Barrier height (top-right) and position of the saddle-point (bottom-right) versus the atomic numbers of heavy nuclei for a given neutron number $N = 128$.

it is in the overlapping part of the fragments ($\xi_{SP} < 1$) for lower values of N starting with $Z = 100$.

REFERENCES

1. C.P. Enz, *No time to be brief (A scientific biography of Wolfgang Pauli)*, Oxford University Press, New York, 2004.
2. L.G. Moretto, Nucl. Phys., **A 247**, 211 (1975).
3. W.D. Myers, W.J. Swiatecki, Nucl. Phys., **A 81**, *1* (1966).
4. W. Scheid, W. Greiner, Z. Phys., **A 226**, 364 (1969).
5. H.J. Krappe, J.R. Nix, A.J. Sierk, Phys. Rev., **C 20**, 992 (1979).
6. D.N. Poenaru, M. Ivaşcu, D. Mazilu, J. Phys. G: Nucl. Phys., **5**, 1093 (1979).
7. D.N. Poenaru, M. Ivaşcu, D. Mazilu, Comp. Phys. Communic., **19**, 205 (1980).
8. D.N. Poenaru, I.H. Plonski, *Nuclear Decay Modes*, Chapter 11, edited by D.N. Poenaru, Institute of Physics Publishing, Bristol, 1996, p. 433.
9. V.M. Strutinsky, Nucl. Phys., **A 95**, 420 (1967).
10. D.N. Poenaru, R.A. Gherghescu, W.Greiner, Phys. Rev., **C 73**, 014608 (2006).

11. D.N. Poenaru, I.H. Plonski, R.A. Gherghescu, W. Greiner, J. Phys. G: Nucl. Part. Phys., **32**, 1223 (2006).
12. R.A. Gherghescu, Phys. Rev., **C 67**, 014309 (2003).
13. R.A. Gherghescu, W. Greiner, Phys. Rev., **C 68**, 044314 (2003).
14. R.A. Gherghescu, W. Greiner, G. Münzenberg, Phys. Rev., **C 68**, 054314 (2003).
15. P. Möller, J.R. Nix, W.D. Myers, W.J. Swiatecki, Atomic Data Nucl. Data Tables, **59**, 185 (1995).